

---

*This copy is for your personal, non-commercial use only.*

---

**If you wish to distribute this article to others**, you can order high-quality copies for your colleagues, clients, or customers by [clicking here](#).

**Permission to republish or repurpose articles or portions of articles** can be obtained by following the guidelines [here](#).

**The following resources related to this article are available online at [www.sciencemag.org](http://www.sciencemag.org) (this information is current as of December 27, 2011):**

**Updated information and services**, including high-resolution figures, can be found in the online version of this article at:

<http://www.sciencemag.org/content/332/6028/451.full.html>

**Supporting Online Material** can be found at:

<http://www.sciencemag.org/content/suppl/2011/03/22/science.1197219.DC1.html>

A list of selected additional articles on the Science Web sites **related to this article** can be found at:

<http://www.sciencemag.org/content/332/6028/451.full.html#related>

This article has been **cited by** 2 articles hosted by HighWire Press; see:

<http://www.sciencemag.org/content/332/6028/451.full.html#related-urls>

This article appears in the following **subject collections**:

Oceanography

<http://www.sciencemag.org/cgi/collection/oceans>

12. M. Ochiai, *Synlett* **2009**, 159 (2009).
13. Ionization potentials of halobenzenes increase in the order PhI (8.69 eV) < PhBr (8.98 eV) < PhCl (9.06 eV) (14).
14. D. R. Lide, Ed., *CRC Handbook of Chemistry and Physics* (CRC Press, Boca Raton, FL, 1992).
15. M. Ochiai *et al.*, *J. Am. Chem. Soc.* **129**, 12938 (2007).
16. M. Ochiai, K. Miyamoto, S. Hayashi, W. Nakanishi, *Chem. Commun.* **46**, 511 (2010).
17. Teflon PFA is a perfluoroalkoxy copolymer resin, available from DuPont, Wilmington, Delaware.
18. Materials and methods are available as supporting material on Science Online.
19. D. S. Breslow, M. F. Sloan, N. R. Newburg, W. B. Renfrow, *J. Am. Chem. Soc.* **91**, 2273 (1969).
20. C. Reichardt, *Solvents and Solvent Effects in Organic Chemistry* (Wiley-VCH, Weinheim, Germany, 2003).
21. R. Mello, M. Fiorentino, C. Fusco, R. Curci, *J. Am. Chem. Soc.* **111**, 6749 (1989).
22. D. D. DesMarteau, A. Donadelli, V. Montanari, V. A. Petrov, G. Resnati, *J. Am. Chem. Soc.* **115**, 4897 (1993).
23. B. P. Gómez-Emeterio, J. Urbano, M. M. Díaz-Requejo, P. J. Perez, *Organometallics* **27**, 4126 (2008).
24. K. Chen, A. Eschenmoser, P. S. Baran, *Angew. Chem. Int. Ed.* **48**, 9705 (2009).
25. M. N. Glukhovtsev, C. Canepa, R. D. Bach, *J. Am. Chem. Soc.* **120**, 10528 (1998).
26. E. Nakamura, N. Yoshikai, M. Yamanaka, *J. Am. Chem. Soc.* **124**, 7181 (2002).
27. X. Lin, C. Zhao, C.-M. Che, Z. Ke, D. L. Phillips, *Chem. Asian J.* **2**, 1101 (2007).
28. Small deuterium KIEs of 1.05 and 1.07 for the hydride abstraction reaction of the bridgehead adamantane C–H bond with tert-butyl cation and hydroperoxonium ion were reported (3).
29. S.-M. Au, J.-S. Huang, W.-Y. Yu, W.-H. Fung, C.-M. Che, *J. Am. Chem. Soc.* **121**, 9120 (1999).
30. Y. M. Badiei *et al.*, *Angew. Chem. Int. Ed.* **47**, 9961 (2008).
31. M. Ochiai, N. Tada, T. Okada, A. Sota, K. Miyamoto, *J. Am. Chem. Soc.* **130**, 2118 (2008).
32. T. Okuyama, T. Takino, T. Sueda, M. Ochiai, *J. Am. Chem. Soc.* **117**, 3360 (1995).
33. P. J. Stang, Z. Rappoport, M. Hanack, L. R. Subramanian, *Vinyl Cations* (Academic Press, New York, 1979).

**Acknowledgments:** This work was supported by a Grant-in-Aid for Scientific Research (B) (Japan Society for the Promotion of Science). We thank Central Glass Co., Japan, for a generous gift of BrF<sub>3</sub>.

#### Supporting Online Material

www.sciencemag.org/cgi/content/full/332/6028/448/DC1

Materials and Methods

SOM Text

Figs. S1 to S12

Tables S1 and S2

References

14 December 2010; accepted 4 March 2011

10.1126/science.1201686

## Global Trends in Wind Speed and Wave Height

I. R. Young,\* S. Zieger, A. V. Babanin

Studies of climate change typically consider measurements or predictions of temperature over extended periods of time. Climate, however, is much more than temperature. Over the oceans, changes in wind speed and the surface gravity waves generated by such winds play an important role. We used a 23-year database of calibrated and validated satellite altimeter measurements to investigate global changes in oceanic wind speed and wave height over this period. We find a general global trend of increasing values of wind speed and, to a lesser degree, wave height, over this period. The rate of increase is greater for extreme events as compared to the mean condition.

Oceanic wind speed and wave height help to control the flux of energy from the atmosphere to the ocean (1) and upper ocean mixing (2). Thus, they substantially influence the mechanisms of air-sea interaction (3). Previous attempts to investigate trends in oceanic wind speed and wave height have used ship observations (4–8), point measurements (9), numerical modeling (10–15), or satellite observations (16). Almost all of these studies are regional rather than global. Although there is a range of results, many studies show an increasing trend in significant wave height, particularly in the North Atlantic and North Pacific, often correlated with interannual variations such as the North Atlantic Oscillation. Careful ship observations (4–6) also show waves locally generated by the wind (hereafter referred to as wind-sea) and swell behaving quite differently and that there exist quite different trends in wind speed and wave height. The present analysis uses recently developed satellite altimeter data sets to carefully investigate such trends on a global scale.

Satellite-based systems provide an alternative to visual or in situ measurements of oceanic wind

speed and wave height, using a variety of instruments, including altimeters, scatterometers, and synthetic aperture radar, providing global coverage of wind and/or waves. Of these instruments, the radar altimeter provides by far the longest-duration record. Since the launch of GEOSAT in 1985, there exists an almost continuous (there was a break in 1990–1991) record of measures from a total of seven different altimeter missions. Numerous calibrations of these altimeters have shown that the instruments can be used to measure significant wave height,  $H_s = 4\sqrt{E}$ , where  $E$  is the total energy of the wave field, with a root mean square (rms) error of less than 0.2 m (17), and wind speed,  $U_{10}$ , with a rms error of less than 1.5 m/s (17–21). Data from altimeter missions have been used to investigate mean ocean wind and wave climatology (21, 22) on a global scale. Recently, Zieger *et al.* (20) carried out systematic calibrations and cross-platform validations of all altimeter measurements over the full 23 years for which data are available. This study provided a consistent data set over this extended period. Because the data set spans multiple satellite platforms, consistent calibration and validation are critical when investigating long-term trends. In the present study, we used this data set to investigate whether there have been systematic changes in the ocean wind and wave climate over this

period. Because the seasonal cycle typically is large, care must be exercised in determining trend information from the data set [supporting online material (SOM)].

We aim here to determine whether there is a statistically significant trend [where trend is defined as a linear increase or decrease in the mean (23, 24)] within the time series of monthly mean, 90th-, and 99th-percentile values of wind speed and wave height for  $2^\circ \times 2^\circ$  regions covering the globe. In the analysis, we take particular care to ensure that the trend can be separated from the seasonal component (SOM).

The trend was quantified as a linear function over the duration of the time series. The analysis revealed that 90th- and 99th-percentile wind speed data from the GEOSAT altimeter were of questionable quality (SOM). Therefore, these data were excluded from the analysis. As a result, the wave height analysis considers the period 1985–2008, whereas wind speed is analyzed for the shorter period 1991–2008. The trend was expressed for each  $2^\circ \times 2^\circ$  region as the annual percentage increase or decrease relative to the mean condition and in absolute terms. The monthly mean, 90th-, and 99th-percentile trend values for both wind speed and wave height are shown in Figs. 1 to 3 (percentage increase or decrease) and Figs. S7 to S9 (SOM) (absolute increase or decrease), respectively.

There is a clear global increase in wind speed for all three statistics. The mean and 90th-percentile wind speed trends are relatively similar, with the magnitude of the increase being larger for the 99th percentile. Such a result indicates that the intensity of extreme events is increasing at a faster rate than that of the mean conditions. At the mean and 90th percentile, wind speeds over the majority of the world's oceans have increased by at least 0.25 to 0.5% per year (a 5 to 10% net increase over the past 20 years). The trend is stronger in the Southern Hemisphere than in the Northern Hemisphere. The only significant exception to this positive trend is the central north Pacific, where there are smaller localized increases in wind speed of approximately 0.25%

Swinburne University of Technology, Melbourne, Victoria, Australia.

\*To whom correspondence should be addressed. E-mail: ir.young@anu.edu.au

per year and some areas where there is a weak negative trend.

Also shown (Figs. 1 to 3) are regions of the globe where the calculated trend is statistically significant at the 95% level (SOM). The calculated wind speed trend for the majority of the globe is statistically significant, the exceptions being the areas of weak positive trend noted above, particularly in the north Pacific.

At the 99th percentile, the wind speed trend becomes more positive, indicating that extreme wind speeds are increasing over the majority of the world's oceans by at least 0.75% per year. The region in the central north Pacific, which showed a weak increasing trend for the mean and 90th percentile, now shows a stronger trend of approximately 0.50% per year, this trend now being statistically significant.

The mean wave height trend (Fig. 1) shows a relatively neutral condition. Large regions of the north Pacific and north Atlantic show a weak negative trend (0.25% per year), as does much of the equatorial regions of all oceanic basins. However, the Southern Hemisphere has a consistent weak positive trend of approximately 0.25% per

year. In almost none of these regions, however, is the trend statistically significant (SOM). The 90th-percentile (Fig. 2) and the 99th-percentile (Fig. 3) wave height trends are progressively more positive, with the higher latitudes (greater than  $\pm 35^\circ$ ) of both the hemispheres showing positive trends of approximately 0.25% per year at the 90th percentile and 0.50% at the 99th percentile. The equatorial and tropical regions of all oceanic basins show a neutral trend for wave height in both cases. The wave height trend becomes more positive moving from the mean to the 99th percentile (i.e., moving to more extreme conditions). It should be noted that the areas of weak trends observed for the mean and 90th percentile are largely not statistically significant. For the 99th-percentile wave height, the stronger positive trends at high latitudes are statistically significant, whereas the weaker trends in the equatorial regions are not. Averaged over the full globe, the following percentages of points produced trends that were statistically significant at the 90/95% confidence levels, respectively: wind speed, 48/36% (mean), 53/40% (90th percentile), 68/55% (99th percent-

ile); wave height, 15/8% (mean), 20/12% (90th percentile), 60/47% (99th percentile).

In order to validate the trends observed in the altimeter data, the same analysis was applied to the 12 deep-water buoys used by Zieger *et al.* (20). The results are shown in Table 1, together with the corresponding altimeter values for  $2^\circ \times 2^\circ$  regions centered on each of the buoy locations. It is clear that there is variability between buoys in the same geographic region and between buoy and corresponding altimeter trend values. However, the same general features observed in the altimeter trends are repeated in the buoy data. At every buoy location, the wind speed trend is positive for each of the monthly mean, 90th-, and 99th-percentile time series. The magnitude of the trend also increases at extreme values, which is consistent with the altimeter results. As for the altimeter observations, there is no clear trend for mean monthly wave height across the buoys. However, the buoys produce a more positive trend for wave height at extreme values, this trend being weaker than for wind speed, again consistent with the altimeter results.

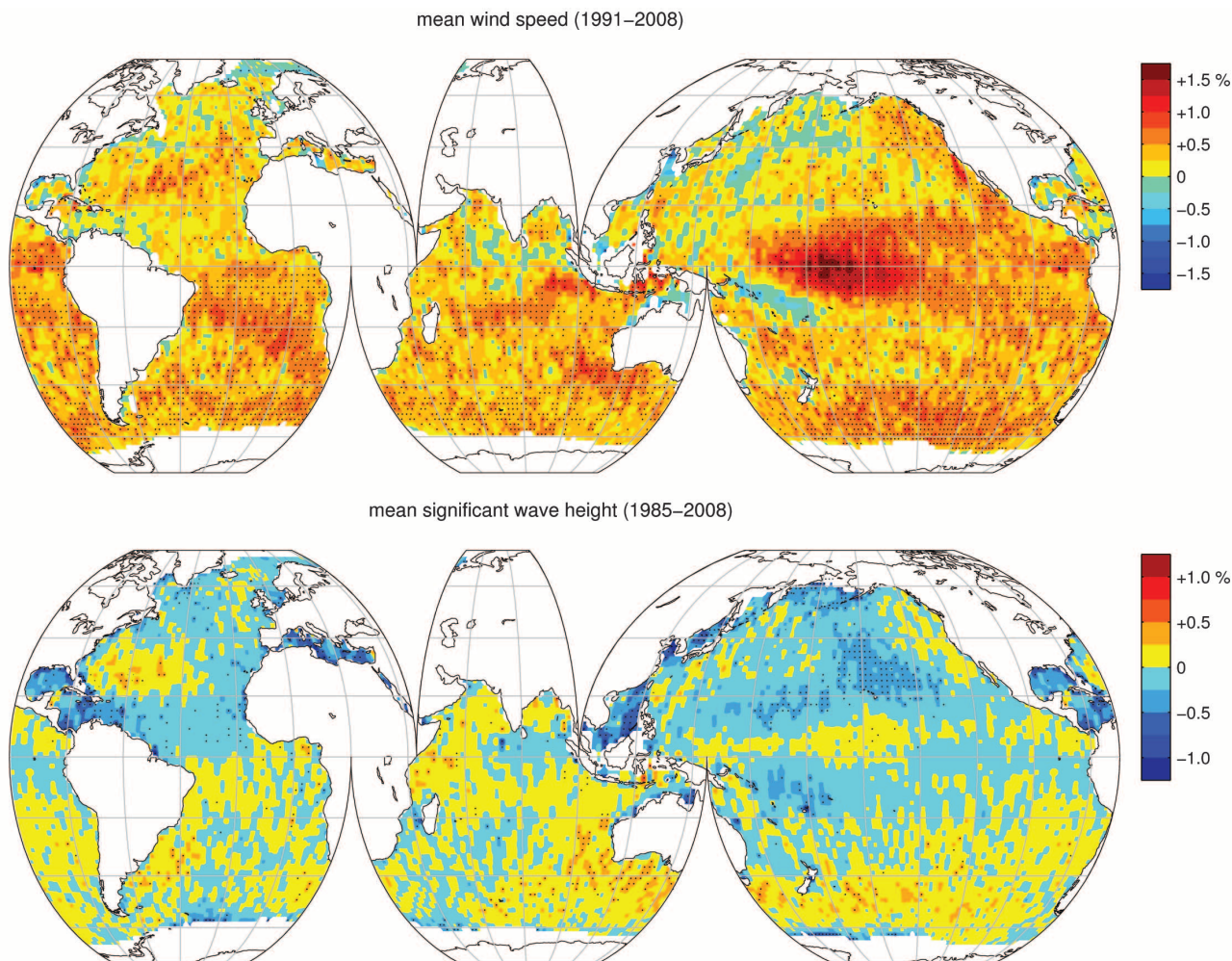


**Fig. 1.** Color contour plots of mean trend (percent per year). Wind speed is shown at the top and wave height at the bottom. Points that are statistically significant according to the Seasonal Kendall test are shown with dots.

A further validation check was performed by comparing the altimeter global trend values with numerical model results. Figure S6 (SOM) shows the trend in mean monthly wind speed calculated from NCEP (National Centre for Environmental Protection) global reanalysis results (25). This result is qualitatively consistent with Fig. 1.

The present analysis cannot absolutely determine why there is a stronger trend in wind speed than in wave height or the underlying physical processes responsible for the observed positive trends in both quantities at extreme values. Observations of local wave generation (26, 27) indicate that for wind-generated waves, significant wave height is approximately proportional to wind speed. Hence, one might initially expect that the spatial patterns for wind speed and wave height would be similar. However, the situation is more complex in that wave height in the open ocean is a mix of locally generated wind-sea and remotely generated swell. Although trends in wind-sea will be correlated with trends in the local wind speed, it has been shown that swell is influenced by not only the intensity of generating meteorological systems but also their frequency (4, 6). Hence, differing trends in wind-sea (a proxy for wind speed) and swell are plausible.

The present results do show causal relationships between the trends in wind speed and wave height. The Southern Ocean is dominated by strong westerly winds blowing across large oceanic fetches. As expected, in this region, there are well-correlated positive trends in both wind speed and wave height. The same is true in the high latitudes of the Northern Hemisphere. In contrast, the wave climate in tropical regions is dominated by remotely generated swell, and the results show little correlation between wind speed and wave height trends in these areas. For extreme conditions (e.g., 99th percentile), waves tend to be generated by local storm events, and hence one would expect a stronger correlation between wind speed and wave height. The present results (Fig. 3 and fig. S9) are consistent with this hypothesis, with wind speed and wave height showing similar positive trends for 99th-percentile conditions.

A detailed analysis of the observed trends would require information on the distribution of

wind-sea and swell together with swell propagation direction and a basin-specific analysis. Such data are not directly available from the altimeter.

The present analysis is aimed at determining whether there is a linear trend over the period of the observations (approximately 23 years). It does not necessarily follow that the observed trends are a result of, for instance, global warming. Indeed, interannual-to-decadal variations of the high-latitude wind belts have been observed, and Hemer *et al.* (28) have shown that the wave climate in the Southern Hemisphere is influenced by the Southern Annular Mode. A regression analysis between the monthly mean altimeter significant wave height and the Southern Annual Mode Index showed a weak correlation, with a correlation coefficient up to 0.4 across large areas of the Southern Ocean. Similar interannual variations have also been shown to be correlated with wave heights in the North Atlantic (5, 10, 11, 13, 14). Hence, it is highly likely that such long-term oscillations will significantly influence the global ocean wind and wave climate. Because the present data set is only two decades long, it is

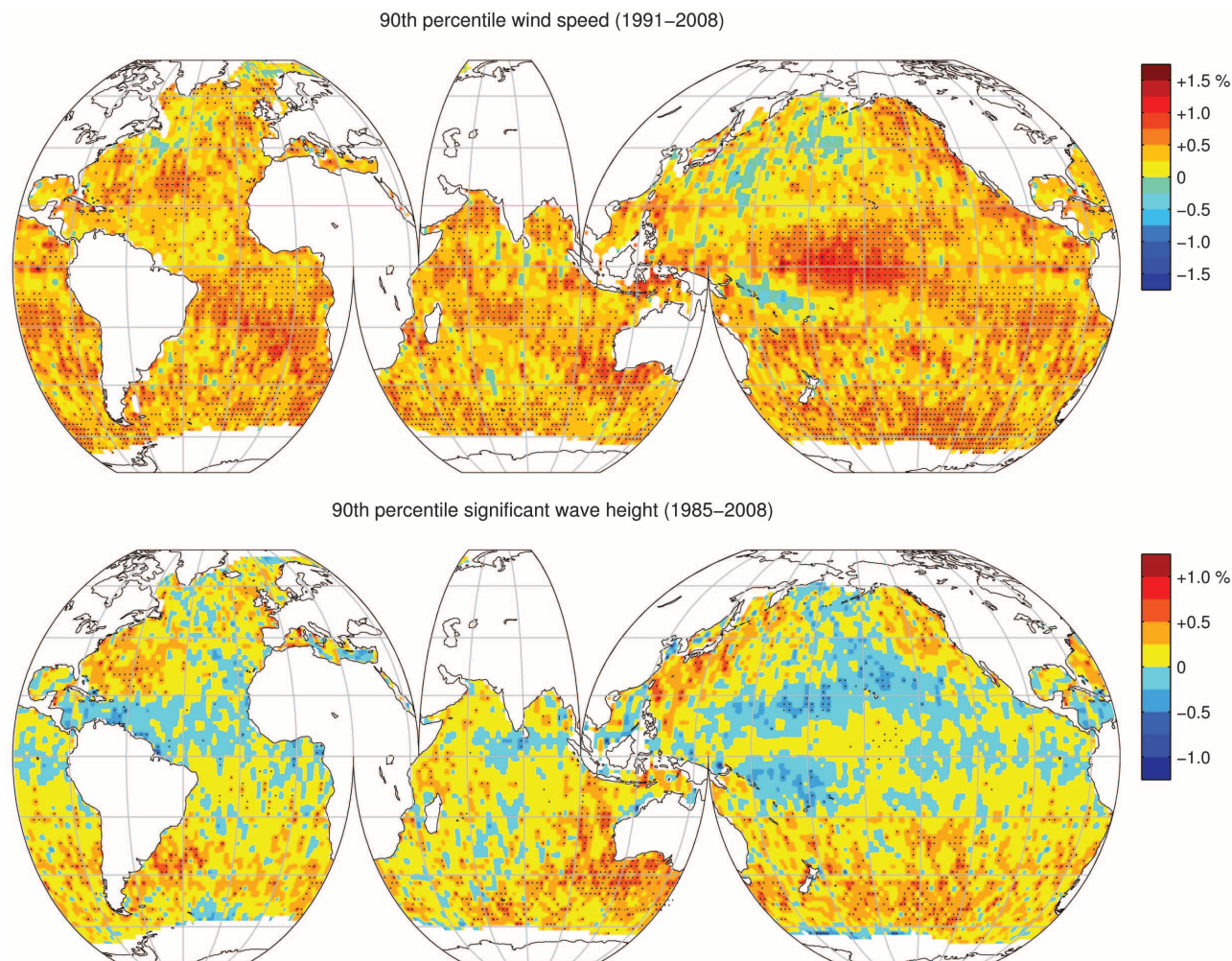


**Fig. 2.** Color contour plots of the 90th-percentile trend (percent per year). Wind speed is shown at the top and wave height at the bottom. Points that are statistically significant according to the Seasonal Kendall test are shown with dots.

**Fig. 3.** Color contour plots of the 99th-percentile trend (percent per year). Wind speed is shown at the top and wave height at the bottom. Points that are statistically significant according to the Seasonal Kendall test are shown with dots.

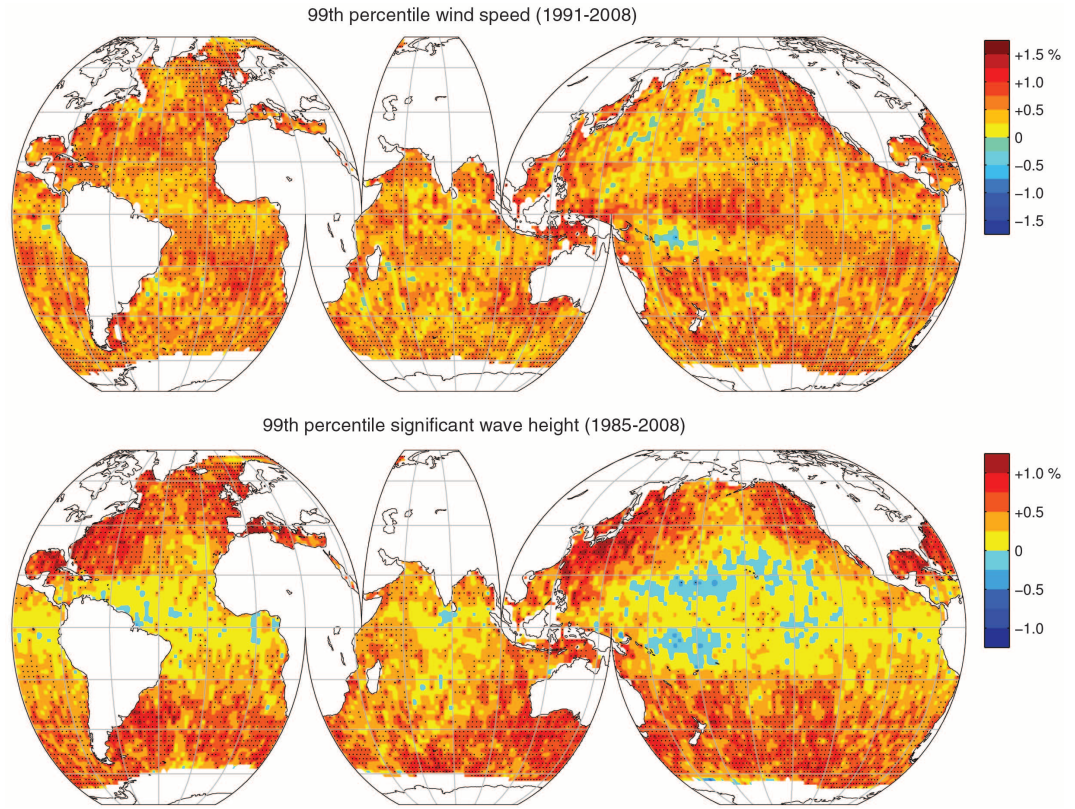


**Table 1.** Comparison of trend estimates for buoy and altimeter data. The top panel shows wind speed and the bottom panel shows wave height, with the locations grouped by geographic region. Bold values are statistically significant at the 95% level (bold and underscored) and at the 90% level (bold) where two significance tests were passed (the normal distribution and the homogeneity test) (SOM).

| Region         | Buoy no. | Latitude (°N) | Longitude (°W) | Buoy trend (cm/s/year) |                     |                     | Altimeter trend (cm/s/year) |                     |                     |
|----------------|----------|---------------|----------------|------------------------|---------------------|---------------------|-----------------------------|---------------------|---------------------|
|                |          |               |                | Mean                   | 90th                | 99th                | Mean                        | 90th                | 99th                |
| Gulf of Mexico | 42001    | 25.9          | 89.7           | 1.79                   | <b><u>3.00</u></b>  | <b><u>4.53</u></b>  | 0.57                        | <b><u>4.50</u></b>  | <b><u>10.11</u></b> |
|                | 42002    | 25.8          | 93.7           | 1.88                   | <b><u>3.07</u></b>  | <b><u>6.29</u></b>  | 1.13                        | 0.00                | 0.69                |
| North Atlantic | 44004    | 38.5          | 70.4           | <b><u>4.01</u></b>     | <b><u>4.42</u></b>  | <b><u>7.34</u></b>  | 0.57                        | 2.41                | <b><u>10.94</u></b> |
|                | 44011    | 41.1          | 66.6           | 0.48                   | 2.46                | 4.63                | 0.51                        | 2.16                | <b><u>13.03</u></b> |
| North Pacific  | 41002    | 32.4          | 75.4           | <b><u>3.66</u></b>     | <b><u>7.50</u></b>  | <b><u>12.99</u></b> | -0.47                       | 2.21                | <b><u>10.73</u></b> |
|                | 46001    | 53.3          | 148.0          | <b><u>2.90</u></b>     | <b><u>4.93</u></b>  | <b><u>7.56</u></b>  | <b><u>5.33</u></b>          | <b><u>7.46</u></b>  | <b><u>10.54</u></b> |
| North Pacific  | 46002    | 42.6          | 130.5          | <b><u>1.99</u></b>     | 2.14                | 2.83                | <b><u>3.24</u></b>          | <b><u>5.25</u></b>  | <b><u>10.42</u></b> |
|                | 46005    | 46.1          | 131.0          | <b><u>4.02</u></b>     | <b><u>6.43</u></b>  | <b><u>8.89</u></b>  | <b><u>4.26</u></b>          | <b><u>5.50</u></b>  | <b><u>13.76</u></b> |
|                | 46006    | 40.9          | 137.5          | <b><u>3.52</u></b>     | <b><u>4.15</u></b>  | <b><u>12.70</u></b> | 2.45                        | 3.33                | <b><u>10.04</u></b> |
|                | 46035    | 57.1          | 177.8          | <b><u>5.62</u></b>     | <b><u>10.00</u></b> | <b><u>9.08</u></b>  | 1.06                        | -0.61               | 0.02                |
| Hawaii         | 51001    | 23.5          | 162.3          | 2.86                   | <b><u>3.59</u></b>  | <b><u>4.42</u></b>  | <b><u>3.99</u></b>          | 2.77                | <b><u>4.96</u></b>  |
|                | 51002    | 17.1          | 157.8          | 2.12                   | 1.40                | 0.92                | 2.90                        | 3.63                | <b><u>6.43</u></b>  |
| Gulf of Mexico | 42001    | 25.9          | 89.7           | 0.24                   | 0.00                | <b><u>1.42</u></b>  | -0.41                       | 0.43                | <b><u>2.41</u></b>  |
|                | 42002    | 25.8          | 93.7           | <b><u>0.55</u></b>     | 0.50                | <b><u>1.00</u></b>  | -0.44                       | 0.24                | <b><u>1.46</u></b>  |
| North Atlantic | 44004    | 38.5          | 70.4           | 0.14                   | 0.40                | 1.27                | -0.54                       | 0.51                | <b><u>2.74</u></b>  |
|                | 44011    | 41.1          | 66.6           | <b><u>0.42</u></b>     | <b><u>1.11</u></b>  | <b><u>1.47</u></b>  | 0.34                        | <b><u>1.64</u></b>  | <b><u>5.20</u></b>  |
| North Pacific  | 41002    | 32.4          | 75.4           | -0.05                  | 0.00                | 0.54                | -0.41                       | -0.02               | <b><u>2.82</u></b>  |
|                | 46001    | 53.3          | 148.0          | -0.45                  | 0.00                | 0.50                | 0.08                        | <b><u>1.24</u></b>  | <b><u>3.03</u></b>  |
| North Pacific  | 46002    | 42.6          | 130.5          | 0.06                   | 0.00                | -0.06               | 0.01                        | 0.58                | <b><u>2.59</u></b>  |
|                | 46005    | 46.1          | 131.0          | 0.36                   | 0.00                | 1.84                | 0.42                        | <b><u>1.67</u></b>  | <b><u>4.50</u></b>  |
|                | 46006    | 40.9          | 137.5          | <b><u>0.98</u></b>     | <b><u>1.25</u></b>  | 1.61                | -0.21                       | 0.24                | <b><u>2.64</u></b>  |
|                | 46035    | 57.1          | 177.8          | -0.31                  | <b><u>-0.95</u></b> | <b><u>-2.54</u></b> | -0.36                       | 0.84                | 2.59                |
| Hawaii         | 51001    | 23.5          | 162.3          | <b><u>-0.71</u></b>    | <b><u>-0.71</u></b> | <b><u>-0.65</u></b> | <b><u>-0.88</u></b>         | <b><u>-0.95</u></b> | -0.06               |
|                | 51002    | 17.1          | 157.8          | 0.02                   | 0.00                | -0.51               | -0.16                       | 0.27                | 0.66                |

not possible to distinguish between a steadily increasing or accelerating trend, which could be extrapolated into the future, or simply the upward portion of a multidecadal oscillation. Only a longer data set will be able to separate these possibilities.

The present analysis does, however, indicate that over the past two decades there has been a consistent trend toward increasing wind speeds. For wave height, the results are more complex, with no clear statistically significant trend for mean monthly values. At more extreme conditions, there is a clear statistically significant trend of increasing wave height at high latitudes and more neutral conditions in equatorial regions.

**References and Notes**

1. M. A. Donelan, W. M. Drennan, K. B. Katsaros, *J. Geophys. Res.* **27**, 2087 (1997).
2. A. V. Babanin, *Geophys. Res. Lett.* **33**, L20605 (2006).
3. A. V. Babanin, A. Ganopolski, W. R. C. Phillips, *Ocean Model.* **29**, 189 (2009).
4. S. K. Gulev, L. Hasse, *Int. J. Climatol.* **19**, 1091 (1999).
5. S. K. Gulev, V. Grigoriev, *Geophys. Res. Lett.* **31**, L24302 (2004).
6. S. K. Gulev, V. Grigorieva, *J. Clim.* **19**, 5667 (2006).
7. S. K. Gulev, D. Cotton, A. Sterl, *Phys. Chem. Earth* **23**, 587 (1998).
8. B. R. Thomas, E. C. Kent, V. R. Swail, A. I. Berry, *Int. J. Climate* **28**, 747 (2008).
9. E. Bouws, D. Jannink, G. J. Komen, *Bull. Am. Meteorol. Soc.* **77**, 2275 (1996).
10. X. L. Wang, V. R. Swail, *Clim. Dyn.* **26**, 109 (2006).
11. A. T. Cox, V. R. Swail, *J. Geophys. Res.* **106**, 2313 (2001).
12. A. Sterl, G. J. Komen, P. D. Cotton, *J. Geophys. Res.* **103**, 5477 (1998).

13. X. L. Wang, F. W. Zwiers, V. R. Swail, *J. Clim.* **17**, 2368 (2004).
14. Y. Kushnir, V. J. Cardone, J. G. Greenwood, M. A. Cane, *J. Clim.* **10**, 2107 (1997).
15. F. Vikebø, T. Furevik, G. Furnes, N. G. Kvamstø, M. Reistad, *Cont. Shelf Res.* **23**, 251 (2003).
16. D. K. Woolf, P. G. Challenor, P. D. Cotton, *J. Geophys. Res.* **107**, 9.1 (2002).
17. I. R. Young, *Appl. Ocean Res.* **16**, 235 (1994).
18. P. Queffelec, *Mar. Geol.* **27**, 495 (2004).
19. I. R. Young, *J. Geophys. Res.* **98**, (C11), 20,275 (1993).
20. S. Zieger, J. Vinoth, I. R. Young, *J. Atmos. Ocean. Technol.* **26**, 2549 (2009).
21. I. R. Young, G. J. Holland, *Atlas of the Oceans: Wind and Wave Climate* (Pergmon, Oxford, UK, 1996).
22. I. R. Young, *Int. J. Climatol.* **19**, 931 (1999).
23. S. R. Esterby, *Hydrol. Process.* **10**, 127 (1996).
24. T. Alexandrov, S. Bianconicini, E. B. Dagum, P. Mass, T. S. McElroy, *A Review of Modern Approaches to the Problem of Trend Extraction* (Technical Report RRS2008/03, U.S. Census Bureau, Washington, DC, 2008).
25. E. Kalnay et al., *Bull. Am. Meteorol. Soc.* **77**, 437 (1996).
26. K. Hasselmann, *Deutsch. Hydrogr. Z.* **8** (suppl. A), 12 (1973).
27. I. R. Young, *Wind Generated Ocean Waves* (Elsevier, Oxford, UK, 1999).
28. M. A. Hemer, J. A. Church, J. R. Hunter, *Int. J. Climatol.* **30**, 475 (2010).
29. This research was supported by an Australian Research Council (ARC) Linkage Grant (LP0882422). We gratefully acknowledge the support of the ARC and our industry partner RPS MetOcean.

### Supporting Online Material

www.sciencemag.org/cgi/content/full/science.1197219/DC1  
SOM Text  
Figs. S1 to S9  
Table S1  
References

1 September 2010; accepted 4 March 2011  
Published online 24 March 2011;  
10.1126/science.1197219

# Latitudinal Gradients in Greenhouse Seawater $\delta^{18}\text{O}$ : Evidence from Eocene Sirenian Tooth Enamel

Mark T. Clementz<sup>1,2\*</sup> and Jacob O. Sewall<sup>3\*</sup>

The Eocene greenhouse climate state has been linked to a more vigorous hydrologic cycle at mid- and high latitudes; similar information on precipitation levels at low latitudes is, however, limited. Oxygen isotopic fluxes track moisture fluxes and, thus, the  $\delta^{18}\text{O}$  values of ocean surface waters can provide insight into hydrologic cycle changes. The offset between tropical  $\delta^{18}\text{O}$  values from sampled Eocene sirenian tooth enamel and modern surface waters is greater than the expected 1.0 per mil increase due to increased continental ice volume. This increased offset could result from suppression of surface-water  $\delta^{18}\text{O}$  values by a tropical, annual moisture balance substantially wetter than that of today. Results from an atmospheric general circulation model support this interpretation and suggest that Eocene low latitudes were extremely wet.

The Eocene epoch represents an extremely warm interval in Earth's climate history. Greenhouse gas concentrations were up to five times as high as present-day levels (1, 2), and annual global temperatures during the Early Eocene Climatic Optimum (EECO) at ~50 million years ago (Ma) were as much as 12°C higher than modern values (3–5). From this temperature peak, conditions gradually declined with only a single prolonged interruption in this trend by a respite to warmer conditions during the Middle Eocene Climate Optimum (MECO) (4, 6). The rate of global temperature deterioration increased markedly at the end of the Eocene as the volume of continental ice on Antarctica rapidly increased. This event defines the Eocene-Oligocene boundary and heralded a major shift in Earth's climate state from greenhouse to icehouse conditions.

The warmer temperatures of the Eocene may have promoted a more vigorous hydrologic cycle, where high global temperatures would have led to an increase in the concentration of water vapor in Earth's atmosphere through intensified subtropical evaporation (7–9). Atmospheric circulation pat-

terns and a reduced latitudinal temperature gradient [e.g., (10)] would have limited rainout along a longitudinal trajectory and facilitated the meridional transport of water and, hence, latent heat to the poles, thus producing a warmer and more humid early Paleogene climate state. Current understanding of atmospheric water vapor content in the Eocene has primarily focused on specific time intervals (e.g., Eocene hyperthermal events) and regions (mid- and high latitudes) (9, 11–13), and evidence that these wetter, more humid conditions extended to lower latitudes or throughout the entire Eocene is so far lacking. In addition to characterizing the tropical greenhouse climate, knowledge of the Eocene hydrologic cycle is critical to accurately calculating paleotemperatures from planktonic foraminifera, as changes in evaporation and precipitation will influence the oxygen isotopic composition of seawater and, hence, that of foraminiferal tests.

One means of acquiring more information on the Paleogene hydrologic cycle comes from the examination of latitudinal changes in the oxygen isotopic composition of ocean surface waters ( $\delta^{18}\text{O}_{\text{sw}}$ ; <100 m depth). A stronger and more immediate connection between marine surface waters and the atmosphere heightens the sensitivity of this oceanic layer to changes in regional hydrology (i.e., precipitation and evaporation) (14, 15). Today, meridional gradients in  $\delta^{18}\text{O}_{\text{sw}}$  are a product of latitudinal differences in evaporation

and precipitation and the isotopic fractionation of water vapor by Rayleigh distillation during transport in the atmosphere (16). The net result is that whereas ocean bottom waters (>1000 m depth) maintain salinities and  $\delta^{18}\text{O}$  values that are more or less uniform globally,  $\delta^{18}\text{O}_{\text{sw}}$  values (Fig. 1A) and surface-water salinities (Fig. 1B) can vary significantly with latitude (17). Enhanced evaporation at lower latitudes leads to higher salinities and  $\delta^{18}\text{O}_{\text{sw}}$  values (as much as 2.0‰ greater than bottom waters). In contrast, reduced evaporation and higher precipitation levels at high latitudes result in lower salinities and  $\delta^{18}\text{O}_{\text{sw}}$  values (more than –2.0‰ lower than those for bottom waters). Thus, one might expect that intensification of the hydrologic cycle during the Eocene would affect the magnitude of this meridional gradient in  $\delta^{18}\text{O}_{\text{sw}}$  values and should be recorded in marine isotope records.

Evidence of global climate change through the Cenozoic has primarily come from geochemical and isotopic analysis of marine microfossils, which precipitate their calcite shells, or tests, in isotopic equilibrium with seawater. As the  $\delta^{18}\text{O}$  values of carbonates is also influenced by temperature, reconstruction of Cenozoic  $\delta^{18}\text{O}_{\text{sw}}$  from planktonic microfossils would require an independent measure of temperature [e.g., Mg/Ca,  $\text{TEX}_{86}$ ,  $\text{U}^k_{37}$ ; (2)], which may be costly and time consuming to obtain. Alternatively, stable isotope analysis of biapatite from marine mammals is more appropriate for reconstructing  $\delta^{18}\text{O}_{\text{sw}}$  values (18). As mammals can maintain a constant core body temperature (~37°C), variation in skeletal biapatite  $\delta^{18}\text{O}$  values simply reflects changes in the oxygen isotopic composition of the waters inhabited by these consumers (19–21). Although postburial alteration is a potential complication for stable isotope analysis of fossil vertebrate material, restriction of analyses to tooth enamel, which is much more resistant to the processes of diagenesis than are other bioapatites (e.g., bone, dentin, or scales), can substantially improve the utility of this method. Likewise, sampling biapatite from large marine mammals can also reduce or remove local environmental effects that are an inherent part of coastal environments (e.g., upwelling, enhanced evaporation, or continental runoff). The large home ranges (22, 23) and long life spans of these species mean that their biapatite  $\delta^{18}\text{O}$  values dampen or negate

<sup>1</sup>Department of Geology and Geophysics, University of Wyoming, Laramie, WY 82071, USA. <sup>2</sup>Program in Ecology, University of Wyoming, Laramie, WY 82071, USA. <sup>3</sup>Department of Physical Sciences, Kutztown University, Kutztown, PA 19530, USA.

\*To whom correspondence should be addressed. E-mail: mclemen1@uwyo.edu; sewall@kutztown.edu